Journal of the Neurological Sciences 283 (2009) 2–8

Contents lists available at ScienceDirect

Journal of the Neurological Sciences

journal homepage: www.elsevier.com/locate/jns

# Improved detection of incipient vascular changes by a biotechnological platform combining *post mortem* MRI *in situ* with neuropathology

Lea Tenenholz Grinberg [a,b,c,*], Edson Amaro Junior [d], Alexandre Valotta da Silva [e], Rafael Emidio da Silva [a,b], João Ricardo Sato [f], Denis Dionizio dos Santos [a], Silmara de Paula Pacheco [a], Renata Eloah de Lucena Ferretti [a], Renata Elaine Paraizo Leite [a], Carlos Augusto Pasqualucci [a,g,h], Stefan J. Teipel [j], Wilhelm H. Flatz [i], Brazilian Aging Brain Study Group [1] and Helmut Heinsen [c]

[a] *Aging Brain Project, Department of Pathology, University of Sao Paulo Medical School, Av. Dr. Arnaldo 455, sala 1353-01246903, Sao Paulo, SP, Brazil*
[b] *Instituto Israelita de Ensino e Pesquisa Albert Einstein, Av. Albert Einstein, 627-05651901, Sao Paulo, SP, Brazil*
[c] *Morphological Brain Research Unit, University of Wuerzburg, Josef-Schneider-Strasse 2, 97080,Wuerzburg, Germany*
[d] *Department of Radiology, University of Sao Paulo Medical School, Av. Dr. Enéas de Carvalho Aguiar, 255-05403.001, Sao Paulo, SP, Brazil*
[e] *Department of Biosciences, Federal University of Sao Paulo, Av. Ana Costa 95 CEP 11060-001, Santos, Brazil*
[f] *Center of Mathematics, Computation and Cognition — Federal University of ABC, Santo Andre, SP, Brazil*
[g] *Autopsy Service of Sao Paulo City, University of Sao Paulo, Av. Dr. Enéas de Carvalho Aguiar 250-05403-000 Sao Paulo, SP, Brazil*
[h] *Department of Pathology, University of Sao Paulo Medical School, Av. Dr. Arnaldo 455, 01246903, Sao Paulo, SP, Brazil*
[i] *Department of Psychiatry and Psychotherapy, University Rostock, Gehlsheimer Str. 20, 18147 Rostock, Germany*
[j] *Clinical Radiology, Ludwig-Maximilian University, Grosshadern, Marchioninistr. 15-81377,Munich, Germany*

ARTICLE INFO

Available online 16 March 2009

*Keywords:*
Neuroimaging
MRI
Neuropathology
Autopsy
Correlation
Methods
3D reconstruction
White matter hyperintensities
Leukoaraiosis

ABSTRACT

The histopathological counterpart of white matter hyperintensities is a matter of debate. Methodological and ethical limitations have prevented this question to be elucidated.
We want to introduce a protocol applying state-of-the-art methods in order to solve fundamental questions regarding the neuroimaging–neuropathological uncertainties comprising the most common white matter hyperintensities [WMHs] seen in aging. By this protocol, the correlation between signal features in *in situ*, *post mortem* MRI-derived methods, including DTI and MTR and quantitative and qualitative histopathology can be investigated. We are mainly interested in determining the precise neuroanatomical substrate of incipient WMHs. A major issue in this protocol is the exact co-registration of small lesion in a tridimensional coordinate system that compensates tissue deformations after histological processing.
The protocol is based on four principles: *post mortem* MRI *in situ* performed in a short *post mortem* interval, minimal brain deformation during processing, thick serial histological sections and computer-assisted 3D reconstruction of the histological sections.
This protocol will greatly facilitate a systematic study of the location, pathogenesis, clinical impact, prognosis and prevention of WMHs.



## 1. Introduction

Cerebral small vessel changes and associated lesions contribute to cognitive decline, either in a pure form or associated with neurodegenerative processes [1–8].

These changes cover a wide range of lesions such as: atherosclerosis, lipohyalinosis, venous collagenosis, amyloid angiopathy and cerebral autosomal dominant arteriopathy with subcortical infarcts and leukoencephalopathy (CADASIL) [9,10].

Aging [11–13], hypertension [3,13,14], diabetes [13,15], heart disease [11,13], atherosclerosis [16], baseline level of white matter hyperintensities (WMH) [17] and endothelial dysfunction [18] are independent risk factors for cerebral small vessels changes in the brain. At variance with the major neurodegenerative diseases the former etiopathogenic factors can be monitored and controlled.

High resolution MRI scans in combination with diffusion tensor imaging (DTI) and magnetization transfer ratio (MTR) protocols provide insight into normal brain structure and vascular supply as well as alterations through brain disease *in vivo* [19]. A detailed and universally accepted correlation of neuroimaging changes and underlying small vessels lesions has not yet been established.

WMHs are commonly detected in routine MRI scans. They have been associated with cerebral small vessel changes in several studies [20–22]. Combined MRI-neuropathological studies disclose the

* Corresponding author. Morphological Brain Research Unit of the Psychiatric Clinic, Oberduerrbacher Str. 6, D-97080, Wuerzburg, Germany. Tel.: +49 931 201 76551.
*E-mail address:* leagrinberg@usp.br (L.T. Grinberg).
[1] Brazilian Aging Brain Study Group, University of Sao Paulo Medical School, Av. Dr. Arnaldo 455, sala 1351-01246903, Sao Paulo, SP, Brazil.

0022-510X/$ – see front matter © 2009 Elsevier B.V. All rights reserved.
doi:10.1016/j.jns.2009.02.327

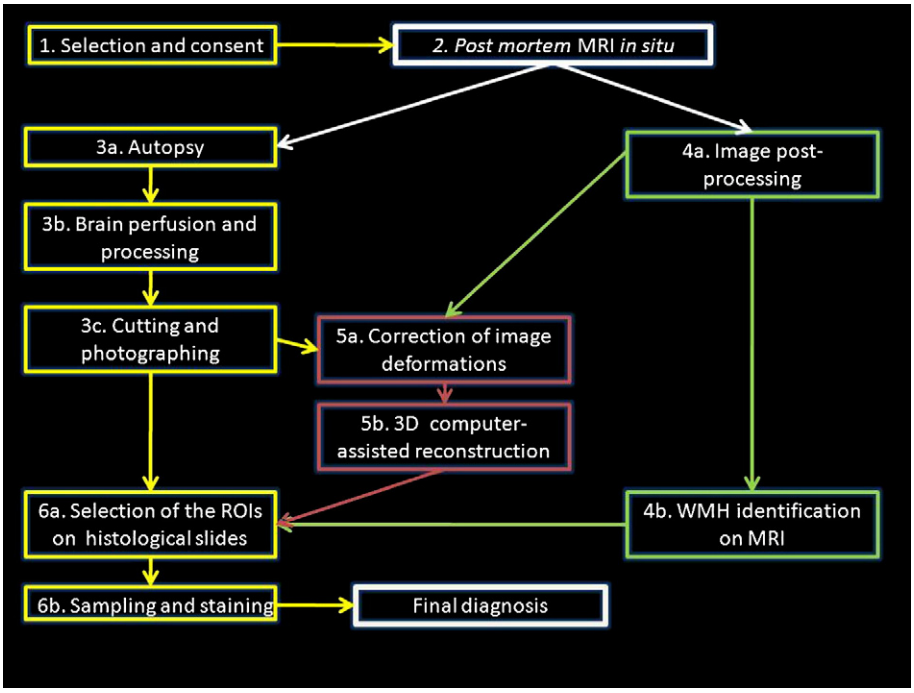


**Fig. 1.** Steps of the protocol for detection of incipient vascular changes by a biotechnological platform combining *post mortem* MRI *in situ* with neuropathology. Note: ROIs — regions of interest.

heterogeneous nature of WMHs, ranging from: ischemic lesions [14,20,23,24], vascular changes [21,25,26], perivascular space enlargement [22,27,28], myelin rarefaction [20,21,29–31], edema [32], denudation of the periventricular lining [28,31,33], gliosis [33,34] and venous collagenosis [35].

Besides all the efforts done so far, the neuropathological substrate of WMHs detected by MRI, has hardly been proven by point-to-point neuroimaging–neuropathological studies, due to methodological and ethical restrictions.

Hence, a number of commonly used diagnostic terms in neuroimaging are based on assumptions. The lack of reliable information about the morphological/neuropathological substrate of such changes limits MRI interpretation and replaces diagnosis by metaphorical terms. These uncertainties limit the use of MRI findings for decisions on treatment of potential cerebrovascular risk factors in elderly patients [33].

Therefore, we want to introduce a protocol applying state-of-the-art methods in order to solve fundamental questions regarding the neuroimaging–neuropathological discrepancies/uncertainties comprising the most common WMHs seen in aging. By this protocol, the correlation between signal features in *in situ post mortem* MRI-derived methods, including DTI and MTR and quantitative histology can be investigated. We are mainly interested in determining the precise neuroanatomical substrate of incipient WMHs. As important advantage, the protocol provides an exact co-registration of small lesions in a tridimensional coordinate system controlled by visual inspection that compensates tissue deformations after fixation and histological processing.

## 2. Methods

This study results of a combination of methods available through a international collaboration among (in alphabetical order): 1) Albert Einstein Research and Education Institute, Sao Paulo; 2) Julius-Maximilian Univ. Wuerzburg — Morphological Brain Research Unit; 3) Ludwig-Maximilian Univ. Munich — Dept. of Psychiatry and Dept. of Radiology; 4) Univ. of Sao Paulo Medical School — Aging Brain Project, Autopsy Service, Dept. of Pathology and Dept. of Radiology.

The study has been approved by the local Ethical committees both in Brazil and Germany.

The protocol comprises 12 steps and is based on four principles: *post mortem* MRI *in situ* performed in a short *post mortem* interval, minimal brain deformation during processing, thick serial histological sections and computer-assisted 3D reconstruction of the histological sections (Fig. 1).

### Step 1. Cases selection and consent

Five *post mortem* brains of cognitively normal subjects were selected from a large group of clinically and pathologically well-characterized cases of the Brazilian Aging Brain Study Group of the University of Sao Paulo Medical School (BBBABSG) [36]. The Informed Consent for brain tissue donation and MRI *in situ* was obtained in each case.

### Step 2. *Post mortem* MRI *in situ*

The cases were scanned at a 1.5 T GE Scanner at the Department of Radiology of the University Sao Paulo Medical School, equipped with 33 mT/m gradients and echo planar capability, within less than 15 h after death.

The acquisition sequences included: T1-weighted volumetric, a T2-weighted and Fluid-attenuated inversion recovery (FLAIR). Diffusion

**Table 1**
Description of the *post mortem* cases used in this study.

| Case number | Age [years] | PMI[a] [h] before MRI | Gender | PMI [h] before autopsy | Clinical diagnosis |
|---|---|---|---|---|---|
| 1 | 78 | 13 | M | 15 | Non-cognitive decline |
| 2 | 77 | 13 | F | 15 | Non-cognitive decline |
| 3 | 42 | 14 | M | 16 | Non-cognitive decline |
| 4 | 62 | 7 | M | 9 | Non-cognitive decline |
| 5 | 62 | 15 | F | 18 | Non-cognitive decline |

[a] *post mortem* interval.

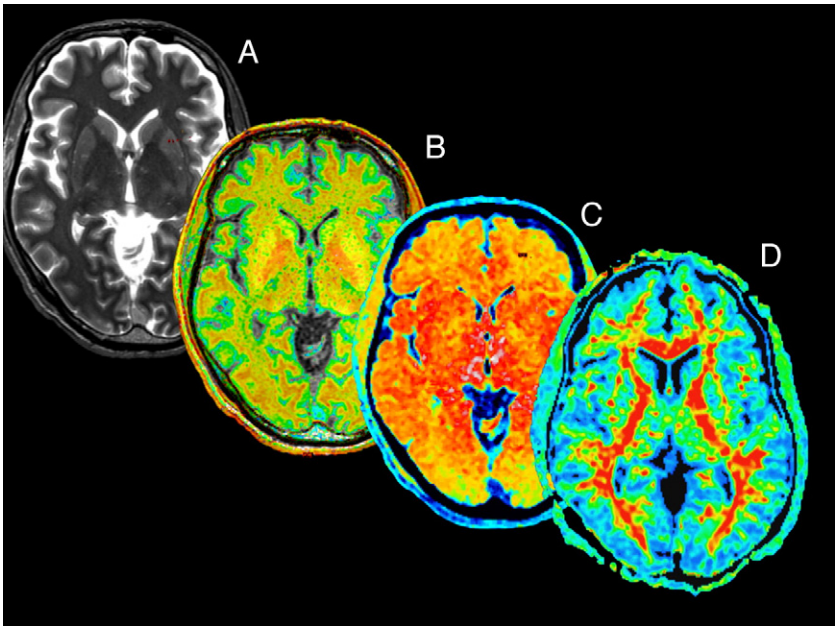


**Fig. 2.** Examples of high quality *post mortem* MRI *in situ*. Brain of a 62 years old male scanned 7 h after death. A) Axial T2-weighted image. B) Corresponding relaxometry map. C) Corresponding magnetization transfer ratio MTR map. D) Corresponding fractional anisotropy map.

tensor images were acquired using an echo-plan3ar gradient echo technique, collecting 43 slices in 25 diffusion coded directions, 6 excitations, and a *b* value of 0 and 1.000.

Step 3a. Autopsy

Brains were removed immediately after the MRI

Step 3b. Brain perfusion and processing

Brains were perfused using mannitol 20% followed by an acetic acid–alcohol–formaldehyde solution and fixed for 4 weeks in a similar solution [37].

After this period, the brains were shipped to Germany, dehydrated in graded series of ethanol solutions and soaked in celloidin for the next steps [38].

Step 3c. Cutting and photographing

The hardened celloidin-embedded blocks were coronally sectioned on a sliding microtome at a thickness of 440 µm. Every second slice was stained with gallocyanin, dehydrated, coverslipped and mounted with Permount® on microscopic slides with a special size of 10×15 cm, as shown in detail by Heinsen et al. [38]. During brain sectioning, the celloidin block was photographed with a digital SLR-camera with close-up lenses, after each slice.

Step 4. WMH identification on MRI

The identification of WMHs was based on the T2, FLAIR and spoiled gradient (SPGR) acquisitions. All lesions were detected as small foci of less than 10 mm with high signal intensity in T2-weighted images. We did not select areas with low T2* intensity, those close to an area of tissue loss (which could suggest an infarct based on radiological findings) or lesions too close to the ventricles.

Step 5a. Correction of image deformations

We have used an automatic registration approach, with minimal user interference. Initially we used manual segmentation in order to extract the extra-cerebral tissue in the MRI images, since automatic algorithm (BET — Oxford University — see below) did not performed to the level of detail necessary for our purposes. A midline cut was done based on the longitudinal section of the corpus callosum and third ventricle. Cerebellum and brain stem (at the level of the junction between midbrain and pons) were also removed. The manual segmentation followed the same approach applied to histological specimen using the software Amira 4.1 (Mercury Computer Systems Inc.). The resultant MRI hemisphere was co-registered to the histological corresponding tissue using affine transformation (12 parameters) implemented in the FLIRT (fMRIB's linear registration tool) from FSL (FMRIB software Library) from Oxford University (http://www.fmrib.ox.ac.uk/fsl/index.html). This step is illustrated in Fig. 3.

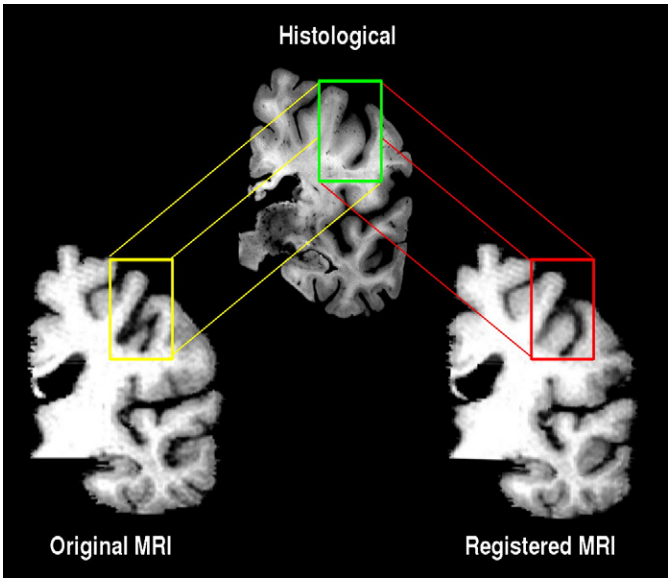


**Fig. 3.** Methods for correcting the histological deformations. Concerning the overall shape there is no perfect correlation between the original MRI and the histological section. The MRI was co-registered to the histological corresponding tissue using affine transformation (12 parameters) implemented in the FLIRT (fMRIB's linear registration tool) from FSL (FMRIB software Library) from Oxford University (http://www.fmrib.ox.ac.uk/fsl/index.html).

Registered images were then analyzed by a neurorradiologist by means of the Osirix software (v3.0) using the resource of multiplanar projection reformatting (Fig. 4). The WMHs were marked in both images.

Step 5b. 3D computer-assisted reconstruction

The photographs of the celloidin block were imported into a computer-assisted 3D reconstruction program (Amira 4.1, Mercury Computer Systems Inc.). Amira converts all the outlines into digital coordinates for generating a surface based upon the individual outlines. Subsequently, each section profile was traced on the digital pictures with the help of a graphic tablet. [39,40].

Step 6a. Selection of the regions of interest [ROIs] on the histological thick sections

The ROIs corresponding to each WMH selected by the radiologists were located point-to-point on the corrected 3D reconstruction of the histological sections.

Step 6b. Sampling and staining

The ROIs were cut out, embedded in paraffin and processed for routine (H&E), special (periodic acid-Schiff, Perls, Verhoff-Van Gieson, Bielschowski, Klüver-Barrera) and immunohistochemical staining (GFAP, CD68, myelin basic protein, neurofilament).

For the immunohistochemical staining, sections (10 μm) were mounted on glass slides and deparaffinised. Subsequently, sections were immersed in 0.3% H2O2 in PBS for 30 min to reduce endogenous peroxidase activity and then blocked in 5% milk. For antigen retrieval, sections were pretreated in 10 mM pH 6.0 citrate buffer and steamed for 30 min. Antibodies were dissolved in 5% milk in PBS. Sections were pre-incubated for 1 h and next incubated with the primary antibodies (4 °C overnight). For the detection of antibodies, commercial ABC-kit (Vectastain Elite, Vector Laboratories, Burlingame, CA) was used according to the instructions of the manufacturer. Color was developed using 3,3'-diaminobenzidine and were counterstained with hematoxylin.

Step 7. Final diagnosis

A neuropathological diagnosis was given to each ROI.

## 3. Results

Our protocol could be successfully applied for all the five cases (data shown on Table 1). The mean processing time from the death to

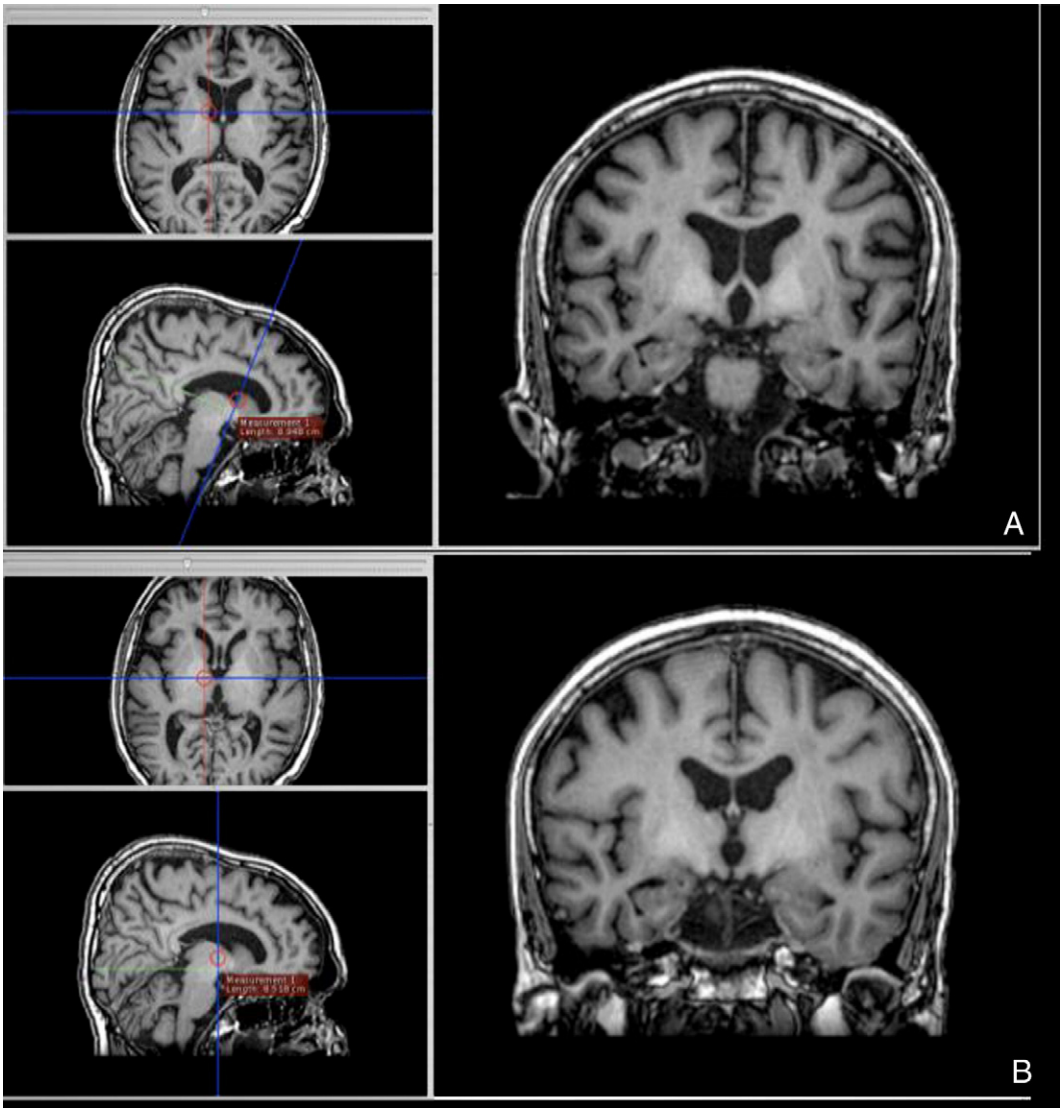


**Fig. 4.** Localization of small WMHs in the original orientation for histological correlation: manual checking. In (A) the position of the histological slice in the MRI image is calculated; and (B) the angle is corrected visually to coincide with the ROI.

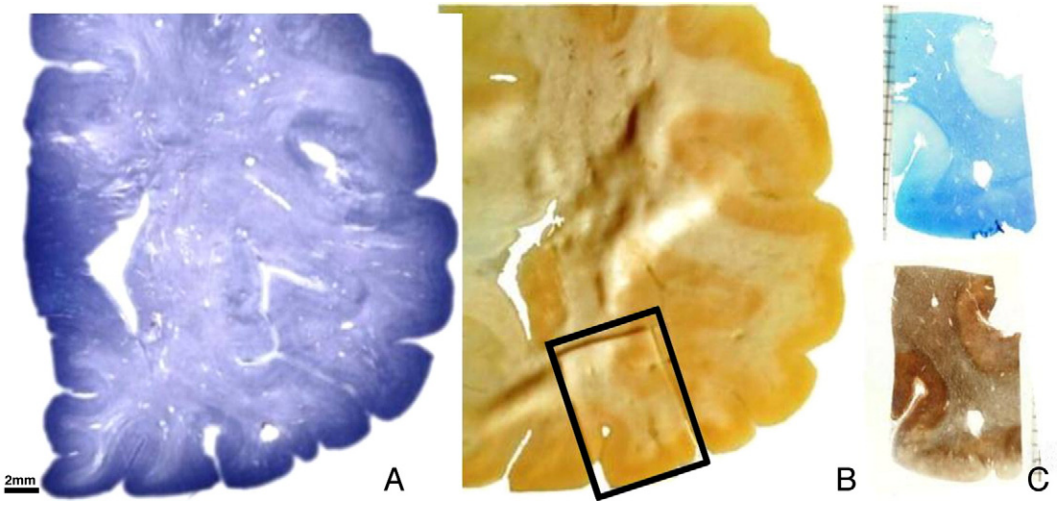


**Fig. 5.** Procedures for sampling the regions of interest (ROIs) on the histological sections. A) Gallocyanin stained 440 μm section. B) Parallel section to A. The tissue segment was cut out, embedded in paraffin and cut in serial 12 μm sections. C) Myelin-stained and axonal stained sections corresponding to the boxed area.

the final data analyses was 4 months: 1 h to the MRI acquisition, 1 h for the autopsy procedure, 3 h for perfusion, three weeks for post-fixation, three weeks for dehydration and embedding, 3 h for cutting, one week for the 3D reconstruction, one week for the immunohistochemical staining and two months for the analyses.

Given the short PMI, the MR signal was very similar to the one expected *in vivo* (Fig. 2).

An example of a MR image registered on a histological slide is shown on Fig. 3. For sampling the ROI, the pathologist was given an image in the original orientation (Fig. 4).

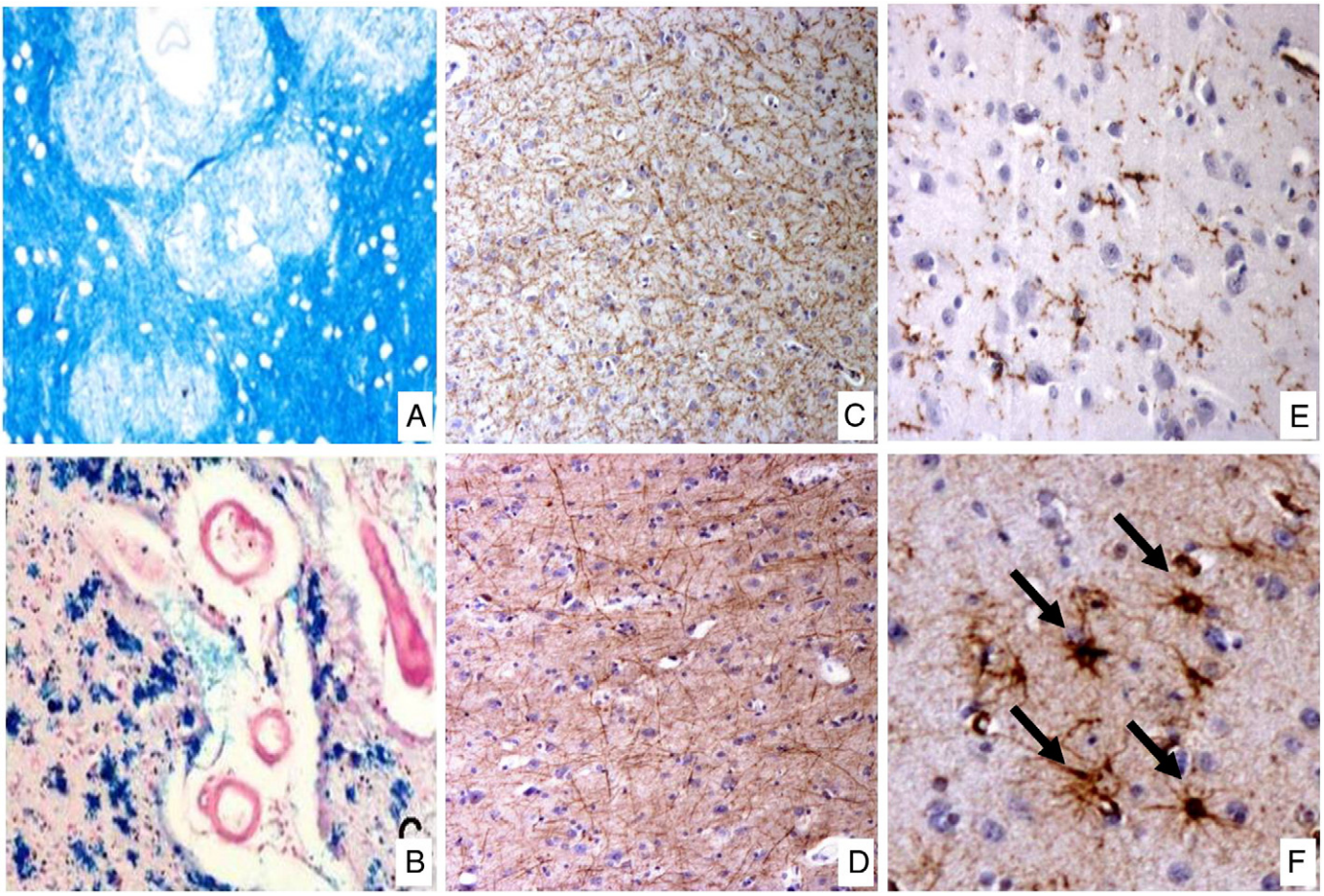


**Fig. 6.** Examples of stainings and immunostainings of the sections through white matter ROIs selected in this study. A) Klüver–Barrera-stained section for myelin. The pallor areas correspond to demyelization. B) Perls-stained section. The blue pigment corresponds to iron accumulation after hemorrhage. C) Myelin basic protein immunostaining (myelinated fibers are stained in golden brown) and D) neurofilament immunostaining. The ROIs are compared to normal areas by optical densitometry. E) CD68 staining for detecting macrophages and microglia (in brown). F) GFAP for detecting reactive astroglia (arrows). (For interpretation of the references to color in this figure legend, the reader is referred to the web version of this article.)

The histological processing was designed to permit further quantitatively and qualitatively assessment, e.g. stereological studies such as: size of the lesion and cellular counting as well as for anatomical location (on the gallocyanin-stained 440um thick sections) and immunohistochemical staining (on the ROIs cut-out of the parallel unstained section). Fig. 5 shows the procedures for sampling the ROIs.

For the histochemical and immunohistochemical assessment, we optimized the most frequently used staining and antibodies for detecting lesions on the brain white matter. All the stainings work very well on paraffin sections. (Fig. 6).

## 4. Discussion

The results of the first correlations support this platform as a reliable, reproducible and feasible tool. Even minimal signal changes can be unequivocally located and can be subjected to a detailed neuropathological diagnosis. We are optimistic that comprehensive future studies on the wrapping procedure will result in fully automatized neuroimaging–neuropathological correlations.

To our knowledge this is one of the first studies to employ *post mortem* MRI *in situ* in humans. Dashner et al. performed a *post mortem* MRI *in situ* in a single case using an 8 T machine [19]. Bendersky et al. compared *post mortem* MRI *in situ* of fetuses with anthropometric measures for evaluating fetal age [41]. However, whilst precise histopathological assessment plays a great role in the present protocol, it has minor importance in the former ones.

Previously methodological limitations have so far prevented other groups from employing *post mortem* MRI *in situ*. We could overcome these limitations by encouraging a multidisciplinary study in which we could maximize the unique facilities of the autopsy service and the department of Radiology of the University of Sao Paulo, e.g. the high number of autopsies performed per day (~50) and the proximity between the two facilities.

Some studies correlate MRI *in-vivo* acquired shortly before death to neuropathology. This approach provides an adequate localization of probable lesions, but pre-agonal factors have a great impact on the brain and it is unlikely that images acquired weeks or months prior to death can be directly correlated with the actual neuropathology of the brain.

Alternatively, the majority of the recent investigations were performed after MRI scanning of *post mortem* formalin-fixed tissue. However, most of the authors report considerable changes in signal intensity of fixed brains [42–44]. In addition, ventricles tend to collapse during fixation. Artifactual ventricular collapse renders the diagnosis of periventricular and deep WMHs difficult. This point is critical because it is assumed that periventricular and deep WMHs differ in pathogenesis, histopathological correlates and prognosis. In our case, the signal obtained from *post mortem* MRI *in situ* was nearly identical to those observed *in-vivo*, although a short *post mortem* delay proved to be essential for acquiring a good image quality and diffusion sequences, as observed by us and other authors [37,45,46].

Tissue deformation cannot be completely prevented during the fixation procedure. This is most frequently observed after immersion fixation in association with unpredictable swelling and shrinking [47]. Taken together, these factors considerably limit correlative imaging/neuropathological studies. In order to avoid these confounding factors, we obtained excellent results after perfusion fixation with mannitol 20% and formalin 20% [37].

Conventional paraffin embedding of complete human brains or hemispheres with subsequent serial sectioning at 20 to 40 μm thickness is time-consuming and expensive [48,49]. We use a modified celloidin method for embedding the brains. Our 400 to 440 μm thick sections are easily handled, have excellent morphological preservation and little deformation. They can be directly compared with the MRI-slices and used for a 3D reconstruction of the sliced brains [50–52]. After gallocyanin staining, fine details and tissue changes down to the cellular level can be diagnosed and verified in parallel unstained sections after paraffin-embedding and neuropathological assessment [38].

Computer-assisted 3D reconstruction is indispensible for the neuroimaging–neuropathologic point-to-point correlation and for correcting linear and non-linear deformations [53]. Also by this mean, the shape and volume of the histopathological lesions can be compared to the MRI findings. It is a matter of debate whether MRI exaggerates non-pathologic changes [54] or the pathological changes are significantly more extensive than the correspondent MRI findings [55]. Our protocol may be used for answering these questions in the future.

So far, this protocol was tested only in a limited number of individuals ranging in age from 50 to 88 years. Nevertheless the excellent cooperation among the research partners in addition to the feasibility and reduced costs of our histological methods greatly facilitate the on-going systematic studies of the location, pathogenesis, clinical impact and prognosis of WMHs.

## Acknowledgments

We would like to acknowledge the brain donors and their families, the autopsy service and Hospital das Clinicas staff and the students from the Brazilian Aging Brain Study Group. We are grateful to Mrs. E.K Broschk for excellent technical assistance and faculty and staff of the Department of Neuropathology of the University of Wuerzburg. Support for this work was provided by Albert Einstein Research Education Institute, FAPESP, Coordenadoria de Apoio ao Pessoal de Nivel Superior—CAPES (Scholarship to LTG and REPL) and Humboldt Foundation (Scholarship to LTG).

## References

[1] Gold G, Kovari E, Hof PR, Bouras C, Giannakopoulos P. Sorting out the clinical consequences of ischemic lesions in brain aging: a clinicopathological approach. J Neurol Sci 2007;257:17–22.
[2] O'Sullivan M, Jones DK, Summers PE, Morris RG, Williams SCR, Markus HS. Evidence for cortical "disconnection" as a mechanism of age-related cognitive decline. Neurology 2001;57:632–8.
[3] Breteler MMB, van Swieten JC, Bots ML, Claus JJ, Grobbee DE, van Gijn J, et al. Cerebral white matter lesions, vascular risk factors, and cognitive function in a population-based study: the Rotterdam Study. Neurology 1994;44:1246–52.
[4] Schmidt R, Fazekas F, Offenbacher H, Dusek T, Zach E, Reinhart B, et al. Neuropsychologic correlates of MRI white matter hyperintensities: a study of 150 normal volunteers. Neurology 1993;43:2490–4.
[5] Ylikoski R, Ylikoski A, Erkinjuntti T, Sulkava R, Raininko R, Tilvis R. White matter changes in healthy elderly persons correlate with attention and speed of mental processing. Arch Neurol 1993;50:818–24.
[6] van der Flier WM, van Straaten EC, Barkhof F, Verdelho A, Madureira S, Pantoni L, et al. Small vessel disease and general cognitive function in nondisabled elderly: the LADIS study. Stroke 2005;36:2116–20.
[7] Longstreth WT, Manolio TA, Arnold A, Burke GL, Bryan N, Jungreis CA, et al. Clinical correlates of white matter findings on cranial magnetic resonance imaging of 3301 elderly people: the cardiovascular health study. Stroke 1996;27:1274–82.
[8] Schmidt R, Petrovic K, Ropele S, Enzinger C, Fazekas F. Progression of leukoaraiosis and cognition. Stroke 2007;38:2619–25.
[9] Kalaria RN, Kenny RA, Ballard CG, Perry R, Ince P, Polvikoski T. Towards defining the neuropathological substrates of vascular dementia. J Neurol Sci 2004;226:75–80.
[10] Munoz DG. Small vessel disease: neuropathology. Int Psychogeriatr 2003(15 Suppl 1):67–9.
[11] Ljindgren A, Roijer A, Rudling O, Norrving B, Larsson E-M, Eskilsson J, et al. Cerebral lesions on magnetic resonance imaging, heart disease, and vascular risk factors in subjects without stroke. A population-based study. Stroke 1994;25:929–34.
[12] Pantoni L, Garcia JH. The significance of cerebral white matter abnormalities 100 years after Binswanger's report. A review. Stroke 1995;26:1293–301.
[13] Lazarus R, Prettyman R, Cherryman G. White matter lesions on magnetic resonance imaging and their relationship with vascular risk factors in memory clinic attenders. Int J Geriatr Psychiatry 2005;20:274–9.
[14] Braffman BH, Zimmerman RA, Trojanowski JQ, Gonatas NK, Hickey WF, Schlaepfer WW, et al. pathologic correlation with gross and histopathology. 2. Hyperintense white-matter foci in the elderly. AJR 1988;151:559–66.
[15] Murray AD, Staff RT, Shenkin SD, Deary IJ, Starr JM, Whalley LJ. Brain white matter hyperintensities: relative importance of vascular risk factors in nondemented elderly people. Radiology 2005;237:251–7.

[16] de Leeuw FE, de Groot JC, Bots ML, Witteman JC, Oudkerk M, Hofman A, et al. Carotid atherosclerosis and cerebral white matter lesions in a population based magnetic resonance imaging study. J Neurol 2000;247:291–6.
[17] Sachdev P, Wen W, Chen X, Brodaty H. Progression of white matter hyperintensities in elderly individuals over 3 years. Neurology 2007;68:214–22.
[18] Hassan A, Hunt BJ, O'Sullivan M, Parmar K, Bamford JM, Briley D, et al. Markers of endothelial dysfunction in lacunar infarction and ischaemic leukoaraiosis. Brain 2003;126:424–32.
[19] Dashner RA, Chakeres DW, Kangarlu A, Schmalbrock P, Christoforidis GA, DePhilip RM. MR imaging visualization of the cerebral microvasculature: a comparison of live and post mortem studies at 8 T. Am J Neuroradiol 2003;24:1881–4.
[20] Fazekas F, Kleinert R, Offenbacher H, Schmidt R, Kleinert G, Payer F, et al. Pathologic correlates of incidental MRI white matter signal hyperintensities. Neurology 1993;43:1683–9.
[21] van Swieten JC, van den Hout JH, van Ketel BA, Hijdra A, Wokke JH, van Gijn J. Periventricular lesions in the white matter on magnetic resonance imaging in the elderly. A morphometric correlation with arteriolosclerosis and dilated perivascular spaces. Brain 1991;114:761–74.
[22] Chimowitz MI, Estes ML, Furlan AJ, Awad IA. Further observations on the pathology of subcortical lesions identified on magnetic resonance imaging. Arch Neurol 1992;49:747–52.
[23] Inzitari D. Age-related white matter changes and cognitive impairment. Ann Neurol 2000;47:141–3.
[24] Pantoni L, Garcia JH. Pathogenesis of leukoaraiosis: a review. Stroke 1997;28:652–9.
[25] Pantoni L, Garcia JH. The significance of cerebral white matter abnormalities 100 years after Binswanger's report. A review. Stroke 1995;26:1293–301.
[26] Sze G, De Armond SJ, Brant-Zawadzki M, Davis RL, Norman D, Newton TH. Foci of MRI signal [pseudo lesions] anterior to the frontal horns: histologic correlations of normal finding. AJR 1986;147:331–7.
[27] Awad IA, Johnson PC, Spetzler RF, Hodak JA. Incidental subcortical lesions identified on magnetic resonance in the elderly. II. Post mortem pathological correlations. Stroke 1986;17:1090–7.
[28] Scheltens P, Barkhof F, Leys D, Wolters EC, Ravid R, Kamphorst W. Histopathologic correlates of white matter changes on MRI in Alzheimer's disease and normal aging. Neurology 1995;45:883–8.
[29] Tomimoto H, Lin J, Ihara M, Ohtani R, Matsuo A, Miki Y. Subinsular vascular lesions: an analysis of 119 consecutive autopsied brains. Eur J Neurol 2007;14:95–101.
[30] Scarpelli M, Salvolini U, Diamanti L, Montironi R, Chiaromoni L, Maricotti M. MRI and pathological examination of post mortem brains: the problem of white matter high signal areas. Neuroradiology 1994;36:393–8.
[31] Takao M, Koto A, Tanahashi N, Fukuuchi Y, Takagi M, Morinaga S. Pathologic findings of silent, small hyperintense foci in the basal ganglia and thalamus on MRI. Neurology 1999;52:666–8.
[32] Munoz DG, Dickson DW, Bergeron C, Mackenzie IRA, Delacourte A, Zhukareva V. The neuropathology and biochemistry of frontotemporal dementia. Ann Neurol 2003;54:S24–8.
[33] Matsusue E, Sugihara S, Fujii S, Ohama E, Kinoshita T, Ogawa T. White matter changes in elderly people: MR–pathologic correlations. Magn Reson Med Sci 2006;5:99–104.
[34] Marshall VG, Bradley WGJ, Marshall CE, Bhoopat T, Rhodes RH. Deep white matter infarction: correlation of MR imaging and histopathologic findings. Radiology 1988;167:517–22.
[35] Moody DM, Thore CR, Anstrom JA, Challa VR, Langefeld CD, Brown WR. Quantification of afferent vessels shows reduced brain vascular density in subjects with leukoaraiosis. Radiology 2004;233:883–90.
[36] Grinberg LT, Ferretti RE, Farfel JM, Leite R, Pasqualucci CA, Rosemberg S, et al. Brain bank of the Brazilian aging brain study group — a milestone reached and more than 1,600 collected brains. Cell Tissue Bank 2007;8:151–62.
[37] Grinberg LT, Amaro E, Teipel SJ, Santos DD, Pasqualucci CA, Leite REP, et al. Assessment of factors that confound MRI and neuropathological diagnosis of human post mortem brain tissue. Cell Tissue Bank 2008;9:195–203.
[38] Heinsen H, Arzberger T, Schmitz C. Celloidin mounting (embedding without infiltration) — a new, simple and reliable method for producing serial sections of high thickness through complete human brains and its application to stereological and immunohistochemical investigations. J Chem Neuroanat 2000;20:49–59.
[39] Grinberg LT, Heinsen H. Computer-assisted 3D reconstruction of the human basal forebrain complex. Dement Neuropsychol 2007;2:140–6.
[40] Heinsen H, Arzberger T, Roggendorf W, Mitrovic T. 3D reconstruction of celloidin-mounted serial sections. Acta Neuropathol 2004;108:374.
[41] Bendersky M, Rugilo C, Kochen S, Schuster G, Sica REP. Magnetic resonance imaging identifies cytoarchitectonic subtypes of the normal human cerebral cortex. J Neurol Sci 2003;211:75–80.
[42] Braffman BH, Zimmerman RA, Trojanowski JQ, Gonatas NK, Hickey WF, Schlaepfer WW, et al. pathologic correlation with gross and histopathology. 1. Lacunar infarction and Virchow–Robin spaces. AJR 1988;151:551–8.
[43] Pfefferbaum A, Sullivan EV, Adalsteinsson E, Garrick T, Harper C. Post mortem MR imaging of formalin-fixed human brain. Neuroimage 2004;21:1585–95.
[44] Boyko OB, Alston SR, Fuller GN, Hulette CM, Johnson GA, Burger PC. Utility of post mortem magnetic resonance imaging in clinical neuropathology. Arch Pathol Lab Med 1994;118:219–25.
[45] Tovi M, Ericsson A. Measurements of T1 and T2 over time in formalin-fixed human whole-brain specimens. Acta Radiol 1992;33:400–4.
[46] D'Arceuil H, de Crespigny A. The effects of brain tissue decomposition on diffusion tensor imaging and tractography. Neuroimage 2007;36:64–8.
[47] Kretschmann HJ, Tafesse U, Herrmann A. Different volume changes of cerebral cortex and white matter during histological preparation. Microsc Acta 1982;86:13–24.
[48] Amunts K, Schleicher A, Burgel U, Mohlberg H, Uylings HB, Zilles K. Broca's region revisited: cytoarchitecture and intersubject variability. J Comp Neurol 1999;412:319–41.
[49] Axer H, Berks G, Keyserlingk DGV. Visualization of nerve fiber orientation in gross histological sections of the human brain. Microsc Res Tech 2000;51(5):481–92.
[50] Teipel SJ, Flatz WH, Heinsen H, Bokde AL, Schoenberg SO, Stockel S, et al. Measurement of basal forebrain atrophy in Alzheimer's disease using MRI. Brain 2005;128:2626–44.
[51] Heinsen H, Hampel H, Teipel SJ. Nucleus subputaminalis: neglected part of the basal nucleus of Meynert — response to Boban et al: computer-assisted 3D reconstruction of the nucleus basalis complex, including the nucleus subputaminalis (Ayala's nucleus). Brain 2006;129:1–4.
[52] Kreczmanski P, Schmidt-Kastner R, Heinsen H, Steinbusch HWM, Hof PR, Schmitz C. Stereological studies of capillary length density in the frontal cortex of schizophrenics. Acta Neuropathol 2005;109:510–8.
[53] Burgel U, Amunts K, Hoemke L, Mohlberg H, Gilsbach JM, Zilles K. White matter fiber tracts of the human brain: three-dimensional mapping at microscopic resolution, topography and intersubject variability. Neuroimage 2006;29:1092–105.
[54] Grafton ST, Sumi SM, Stimac GK, Alvord EC, Shaw CM, Nochlin D. Comparison of post mortem magnetic resonance imaging and neuropathologic findings in the cerebral white matter. Arch Neurol 1991;48:293–8.
[55] Bronge L, Bogdanovic N, Wahlund LO. Post mortem MRI and histopathology of white matter changes in Alzheimer brains. A quantitative, comparative study. Dement Geriatr Cogn Disord 2002;13:205–12.